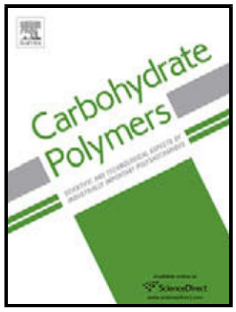

Title: SYNTHESIS AND CHARACTERIZATION OF SUPRAMOLECULAR SYSTEMS CONTAINING NIFEDIPINE, β-CYCLODEXTRIN AND ASPARTIC ACID

Authors: Juan Pablo Cerutti, Mario Alfredo Quevedo, Natalia Buhlman, Marcela Raquel Longhi, Ariana Zoppi

PII: S0144-8617(18)31226-8
DOI: https://doi.org/10.1016/j.carbpol.2018.10.038
Reference: CARP 14170

To appear in:

Received date: 15-8-2018
Revised date: 27-9-2018
Accepted date: 12-10-2018

Please cite this article as: Cerutti JP, Quevedo MA, Buhlman N, Longhi MR, Zoppi A, SYNTHESIS AND CHARACTERIZATION OF SUPRAMOLECULAR SYSTEMS CONTAINING NIFEDIPINE, β-CYCLODEXTRIN AND ASPARTIC ACID, *Carbohydrate Polymers* (2018), https://doi.org/10.1016/j.carbpol.2018.10.038

SYNTHESIS AND CHARACTERIZATION OF SUPRAMOLECULAR SYSTEMS CONTAINING NIFEDIPINE, β-CYCLODEXTRIN AND ASPARTIC ACID

Juan Pablo Cerutti[a], Mario Alfredo Quevedo[a,b], Natalia Buhlman[a], Marcela Raquel Longhi[a,b], and Ariana Zoppi [a,b]

[a]Departamento de Ciencias Farmacéuticas, Facultad de Ciencias Químicas, Universidad Nacional de Córdoba, Córdoba, Argentina.

[b]Unidad de Investigación y Desarrollo en Tecnología Farmacéutica (UNITEFA, CONICET) and Facultad de Ciencias Químicas, Universidad Nacional de Córdoba, Córdoba, Argentina.

***Corresponding author**: Ariana Zoppi. Unidad de Investigación y Desarrollo en Tecnología Farmacéutica (UNITEFA, CONICET). Facultad de Ciencias Químicas. Universidad Nacional de Córdoba. Haya de la Torre y Medina Allende, s/n. Ciudad Universitaria. X5000HUA Córdoba. Argentina. Tel.: +54-351-5353865 fax: +54-351-5353865. E-mail: ariana@fcq.unc.edu.ar

Graphical abstract

HIGHLIGHTS:

- Complexes of nifedipine with β-cyclodextrin and aspartic acid were prepared
- Multicomponent complex formation increase the aqueous solubility of nifedipine
- Complexation showed an improvement of the dissolution profile of the drug
- Nifedipine inserted its aromatic ring into the β-cyclodextrin cavity
- Complexes represent a promising approach to nifedipine formulation optimization

ABSTRACT

The purpose of this work was to characterize complexes of nifedipine with β-cyclodextrin (β-CD), with and without auxiliary agents, to improve aqueous solubility and the dissolution

profile of nifedipine. Complexes were characterized using infrared spectroscopy, thermoanalytical methods, powder X-Ray diffraction, scanning electron microscopy, phase solubility analysis and dissolution studies. Spatial configurations were determined by NMR and further examined using computational techniques. This investigation showed that the amino acid Asp was the most efficient auxiliary agent for multicomponent complexes. The spatial configurations were consistent with those obtained by molecular modelling; evidencing that nifedipine inserted its aromatic ring into β-CD, in all complexes, with Asp interacting with the wide hydrophilic rim of β-CD. The dissolution rates of nifedipine:β-CD:Asp complexes were significantly increased compared to those of the pure drug or nifedipine:β-CD. These results indicate that the nifedipine:β-CD:Asp system is a promising approach for the preparation of optimized formulations of nifedipine.

KEYWORDS: nifedipine; β-cyclodextrin; multicomponent complex; molecular modelling; dissolution studies

1. NTRODUCTION

Enhancing the solubility of poorly water-soluble drugs is one of the most important objectives of the pharmaceutical industry, since limited water solubility is generally associated with suboptimal dissolution profiles and thus poor oral bioavailability (Göke et al., 2018; Kawabata, Wada, Nakatani, Yamada & Onoue, 2011). This is the case of nifedipine (NIF, Fig. 1A), a calcium-channel blocking agent widely used in the treatment of angina pectoris and hypertension. NIF is classified as a class II substance in the biopharmaceutical classification system (BCS), exhibiting poor water solubility while presenting a high permeability. Its pharmacokinetic parameters following oral administration are dependent on the type of dosage form used (Gajendran et al., 2015; Mercuri, Fares, Bresciani & Fotaki, 2016). A very important challenge for researchers is to develop new drug delivery systems in order to increase the solubility and dissolution rate of class II BCS drugs, such as NIF, with the aim of improving dissolution rate profiles leading to enhanced intestinal absorption and the corresponding increased bioavailability.

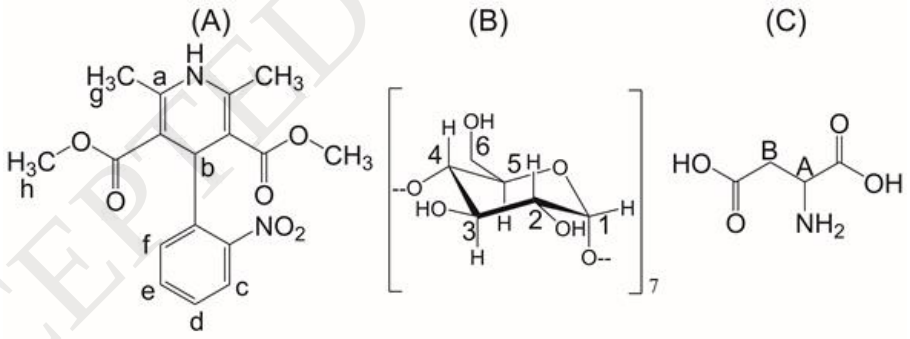

Figure 1. Molecular structure and NMR signal notation of: (A) NIF, (B) β-CD and (C) ASP.

Cyclodextrins (CDs) are cyclic oligosaccharides, widely used in pharmaceutical formulations to enhance the solubility, dissolution rate and bioavailability of drugs. Their truncated cone structure is open at both ends, facilitating the incorporation of organic molecules in its cavity,

and thus efficiently forms inclusion complexes. In the absence of a guest molecule, water molecules from the bulk solution occupy the interior cavity of CDs, thus desolvation events are required prior to ligand inclusion. In addition, as the exterior rims of CDs contain several hydroxyl groups, additional electrostatic interactions with these groups are also possible upon ligand binding. Three types of natural CDs are frequently used in the pharmaceutical industry, namely α-, β- and γ-CD, containing six, seven or eight (α-1-4)-linked D-glucopyranoside units, respectively (Iacovino et al., 2017; Muankaew & Loftsson, 2018; Narayanan, Boy, Gupta & Tonelli, 2017). Among them, β-CD (Fig. 1B) is the most widely used CD, mostly because of the size of its cavity, which is appropriate for the inclusion of a vast number of therapeutically relevant drugs. In addition, β-CD is the cheapest among natural CDs, which is also a significant advantage in the context of bulk material preparations. In previous works, different researchers have investigated the complexation of NIF with CDs, with the aim of overcoming the limitations related to its poor water solubility (Acartürk, Kişlal & Çelebi, 1992; Bayomi, Abanumay & Al-Angary, 2002; Chutimaworapan, Ritthidej, Yonemochi, Oguchi & Yamamoto, 2000; de Araújo et al., 2017; Filipović-Grčić, Bećirević-Laćan, Skalko & Jalšenjak, 1996; Heydari, Iranmanesh, Doostan & Sheibani, 2015; Jagdale, Jadhav, Chabukswar & Kuchekar, 2012; Nikolić et al., 2010; Škalko, Brandl, Bećirević-Laćan, Filipović-Grčić & Jalšenjak, 1996; Uekama, Ikegami, Wang, Horiuchi & Hirayama, 1992). Although some of these results can be considered promising, in terms of biopharmaceutical performance, Beig et al. observed a decrease in the apparent intestinal permeability of NIF, as a function of increasing CD concentrations (Beig, Miller & Dahan, 2013), a feature that may limit the biopharmaceutical performance of the binary system. Several studies carried out by different research groups have established that solubilization and complexation efficiency of CDs can be improved by forming multicomponent complexes, using auxiliary substances, such as polymers, amino acids or hydroxypropylacids (Aiassa, Zoppi, Albesa & Longhi, 2015; Aiassa, Zoppi, Becerra, Albesa & Longhi, 2016; Barbosa et

al., 2014; Vieira et al., 2015). This strategy is of particular interest applied towards enhancing NIF bioavailability, since it allows the use of lower doses of CDs to reach the desired solubilizing effect compared to binary systems. The design of these kinds of multicomponent systems is very promising since they allow formulation costs to diminish while avoiding CD concentration dependent effects (Loftsson & Brewster, 2012).

In this work, we hypothesize that the preparation of multicomponent supramolecular systems of NIF with β-CD and essential amino acids (AAs) may be able to enhance the water solubility and dissolution rate of the drug in a greater extent, compared to that of the binary complex. In this way, different amino acids were screened with respect to their effect in NIF solubility, as a measure of their utility as auxiliary agents. The multicomponent system with the most efficient AA was prepared and studied in detail, including phase solubility analyses, infrared spectroscopy, thermoanalytical methods, powder X-Ray diffraction and scanning electron microscopy. To further, characterize the multicomponent systems at an atomic level, molecular docking and dynamics studies were carried out, along with combined free-energy of binding analyses. Computational findings were consistent with experimental results, finding agreement between spectroscopic (^{1}H NMR) data and the predicted three dimensional structures of the binary and multicomponent complexes. Furthermore, empirical affinity parameters and binding energies were calculated to investigate the stability of all the prepared complexes.

2. MATERIALS AND METHODS

2.1. Materials

Nifedipine (98.7%) and glycine (98%) were purchased from Parafarm. β-CD (MW: 1135 g/mol) was kindly donated by Roquette (agent of Roquette in Argentina); arginine (98%), histidine (99%) and leucine (98%) were purchased from Sigma-Aldrich; aspartic acid (99.3%) from Anedra. Dimethyl sulfoxide-D_6 (99.8%, MagniSolv™) deuterated solvent was

obtained from Merck, while water intended for all analyses was obtained from a Millipore Milli-Q water purification system.

2.2. Selection of Auxiliary Agents

A series of amino acids were screened with NIF to select the appropriate auxiliary agent to prepare multicomponent complexes. Experiments were carried out at 37 °C in stoppered glass tubes containing an excess amount of NIF (10 mg), with addition of 3 mL of aqueous solutions containing a fixed concentration (5mM) of the following amino acids: arginine (Arg), aspartic acid (Asp), glycine (Gly), histidine (His) and leucine (Leu). All suspensions were shaken on a vortex for 15 seconds and placed in a thermostatic bath at 37.0 ± 0.1 °C to reach solubilization equilibria protected from light. Prior to quantification, the samples were filtered using a membrane of 0.45 µm (Millipore, USA) in vials. Quantitative determinations of NIF were performed using an Agilent S1100 High Performance Liquid Chromatography (HPLC) system, equipped with a Phenomenex C8 (4.6 x 250 mm and 5 µm) column at 25°C. The mobile phase was methanol:water (60:40), at a flow rate at 1mL/min. Analyte signals were obtained using an UV detector set at 238 nm.

2.3. Phase solubility analysis

The effect of β-CD on the solubility of NIF was studied in triplicate, in the presence and absence of the corresponding amino acids. Excess amounts of NIF (10 mg) were added in stoppered glass tubes containing water solutions with a fixed concentration of the auxiliary agent (5mM) and different amounts of β-CD (0–12.4 mM). Samples were shaken on a vortex for 15 seconds and then placed in a thermostatic bath at 37.0 ± 0.1 °C to reach solubilization equilibria, protected from light. Prior to quantitation through HPLC, samples were filtered with a membrane of 0.45 µm pore diameter (Millipore, USA) in vials and analysed by HPLC. Phase solubility curves for the binary and multicomponent systems were obtained by plotting

the concentration of solubilized NIF versus β-CD concentration in the sample. The stability constants (K_C) of the complexes were calculated, considering the saturation solubility of NIF (S_0) in water in the absence of β-CD (for the binary complex) or β-CD and AA (for the multicomponent complex). The K_C was calculated from the slope of the phase solubility diagrams (Eq. 1):

$$K_C = \text{slope} / S_0 (1 - \text{slope}) \qquad \text{(Eq. 1)}$$

2.4. Molecular modelling

Initial structures: the structure of β-CD was obtained from the Cambridge Structural Database (code BCDEXD10), while those of the corresponding ligands were constructed from their SMILES nomenclature, using the MarvinSketch software (MarvinSketch, 2017). Prior to docking assays, the three-dimensional structures of the ligands were energy minimized by applying a semiempirical method as implemented in the software Gaussian09 (Frisch et al., 2009).

Molecular docking studies: in order to perform these studies, the Autodock4 software was used (Morris et al., 2009). In all docking procedures, a docking grid was precomputed using the Autogrid4 software, setting a docking grid positioned in the centre of mass of β-CD, and extending 22 Å in the x,y,z direction. The charges corresponding to β-CD were assigned from the Glycam06 force field (Kirschner et al., 2008), while those for the ligand were assigned from the GAFF forcefield (Wang, Wolf, Caldwell, Kollman & Case, 2004). Docking runs were performed considering a rigid receptor (i.e. β-CD) and a flexible ligand, with the corresponding conformations generated using a Lamarckian Genetic Algorithm applying the default search parameters implemented in the software. To exhaustively analyse the resulting docked poses, a representative member of each cluster of conformations obtained from the docking runs was subjected to further analysis by molecular dynamics (MD), both for the binary and multicomponent systems. To obtain the multicomponent complex; the

starting structure of the corresponding binary complex was generated from a cluster analysis applied over the molecular dynamics trajectories obtained for each NIF binding mode. As was performed for the binary system, to identify the most stable binding mode of the auxiliary agent, all alternate binding modes were subjected to MD analysis and free energy of binding analysis.

Molecular Dynamics simulations: The Amber18 software was used (Case et al., 2018), using explicit solvent conditions to obtain each trajectory. Starting structures corresponding to either the binary or multicomponent complex were parameterized using the *tleap* module of Amber18 (Case et al., 2018), applying the corresponding parameters form the *Glycam06* and *GAFF* forcefields for the host and guest molecules, respectively (Kirschner et al., 2008; Wang, Wolf, Caldwell, Kollman & Case, 2004). Complexes were solvated using a pre-equilibrated TIP3P explicit water model, applying a solvent box with boundaries at a minimum distance from the solute of 10 Å in each direction. After standard minimization procedures (5000 steps, first stage: solute restrained; 5000 steps, second stage: unrestrained system), the minimized complexes were heated under constant volume conditions from 0 to 300 K in a 0.5 ns timeframe, applying restraints on the solute. Next, the complexes were equilibrated during 1 ns, after which the production phase under constant pressure and temperature conditions was performed for an additional 10 ns. In all cases, a 2 fs timestep was used, with the SHAKE algorithm applied to constrain all covalent bonds involving hydrogen atoms. A 10 Å cutoff value was used to calculate non-bonded interactions. In addition, MD simulations were also studied using DMSO as explicit solvent. To develop the solvent system, DMSO charges were calculated using *ab-initio* methods as implemented in the Gaussian 09 software (Frisch et al., 2009), after which a 60 Å DMSO cubic box was constructed using the Packmol software (Martínez, Andrade, Birgin & Martínez, 2009). The corresponding box of solvent was pre-equilibrated at 300K applying standard MD protocols, considering a successful equilibration once the experimental density

value for DMSO was reached (1.1 g/cm^3). Periodic boundary properties were assigned to the developed DMSO box in order to simulate the corresponding systems.

MD trajectories were generated using CUDA designed code (pmemd.cuda), and computed using computational resources provided by the CCAD – Universidad Nacional de Córdoba (http://ccad.unc.edu.ar/). In particular, the Mendieta cluster was used, which is part of SNCAD – MinCyT, República Argentina.

Energetic interaction studies: The *Molecular Mechanics Generalized Born Surface Area* technique (Miller, McGee, Swails, Homeyer, Gohlke & Roitberg, 2012) was used to calculate the interaction energies corresponding to molecular docking poses and MD trajectories obtained for each binding mode and cluster of conformations.

Analysis and visualization: MD trajectories were displayed using the VMD software (Humphrey, Dalke & Schulten, 1996) and were analysed with CPPTRAJ module of Amber18. Some specific processes were performed using in-house developed scripts.

2.5. Nuclear Magnetic Resonance spectroscopy (^{1}H NMR)

The ^{1}HNMR studies were carried out to characterize the interaction mechanism of NIF with both β-CD and Asp. All NMR spectra were collected using a BrukerAvance II High Resolution spectrometer at 400.16 MHz. Samples were dissolved in DMSO-d_6. Induced changes in the ^{1}H chemical shifts of NIF, β-CD and AA, originated due to their complexation, were calculated using equation 2:

$$\Delta\delta = \delta_{complex} - \delta_{free} \qquad \text{(Eq. 2)}$$

2.6. Preparation of systems in the solid state

Binary (NIF:β-CD) and multicomponent systems (NIF:β-CD:AA) were prepared by two mechanochemical methods.

Physical Mixing (PM): binary and multicomponent systems were prepared employing 1:1 molar ratio of NIF:β-CD and 1:1:1 molar ratio of NIF:β-CD:AA. Both preparations were mixed in an agate mortar for 5 min and were stored in glass vials protected from light.

Kneading (KN): NIF, β-CD and AA with 1:1 and 1:1:1 molar ratio were accurately weighed and transferred to a mortar, adding 0.25 µL of a methanol:water (1:1vol./vol.) mixture per mg of solid and the mixture was kneaded in a mortar for 30 min until an homogenous paste was formed. In addition, pure NIF was processed following the same protocol for comparative purposes. All samples were stored in glass vials protected from light.

2.7. Infrared Spectroscopy (IR)

The IR spectra of pure compounds, binary and multicomponent systems (both obtained by physical mixtures and kneading) were recorded on a Nicolet Avatar 360 FTIR spectrometer in the range of 4000-400 cm^{-1}.

2.8. Differential Scanning Calorimetry and Thermogravimetry

Differential scanning calorimeter (DSC) tests were recorded on a DSC Discovery series instrument (TA, USA) and thermogravimetric (TG) tests of samples were recorded on a TG Discovery series instrument (TA, USA). The thermal behaviour was studied by heating 1-2 mg of the samples in perforated aluminium capsules under nitrogen atmosphere, scanning a temperature range between 25-200°C (DSC) and 25-350°C (TG), applying a heating rate of 10°C min^{-1}. The relative degree of drug crystallinity (RDC) in the complexes was calculated using equation 3:

$$\mathrm{RDC} = \frac{\Delta H_{complex}}{\Delta H_{drug}}\, x\, 100 \qquad \text{(Eq. 3)}$$

Where $\Delta H_{complex}$ correspond to the fusion enthalpy of NIF in the complex and ΔH_{drug} corresponds to the fusion enthalpy of pure NIF.

2.9. Powder X-Ray Diffraction (PXRD)

The PXRD patterns were recorded at room temperature on a PANanalitycal X'Pert PRO diffractometer with Cu-Kα radiation. The PXRD data were collected by scanning 2θ from 4° to 35° with a step size of 0.026° at a scanning rate of 23.0 s/step.

2.10. Scanning Electron Microscopy (SEM)

The SEM microphotographs were collected using a Carl Zeiss Σigma microscope at the Laboratorio de Microscopía y Análisis por Rayos X (LAMARX) of the Universidad Nacional de Córdoba, Argentina. The samples were fixed on a brass stub using double-sided aluminium tape, which were then made electrically conductive by coating in gold under vacuum using a Quorum 150 sputter coater.

2.11. Dissolution study

To investigate the effect of complexation of NIF on its dissolution behaviour, studies were performed using a dissolution apparatus (Hanson SRII6 Flask Dissolution Test Station, Hanson Research Corporation, Chatsworth, USA). Assays were carried out using an equivalent of 10 mg of NIF (in powder state) and 900 mL of simulated gastric fluid, free of enzymes (pH 1.2). The dissolution medium was maintained at 37.0 ± 0.5 °C and stirred at 50 rpm. Aliquots (2 mL) were collected at predetermined time intervals and filtered using 0.45 μm pore diameter membranes (Millipore, USA). Equal volumes of pre-warmed fresh dissolution medium were used to replace the volume corresponding to withdrawn samples. The filtered sample solutions were analysed using a UV spectrophotometer (Shimadzu, UV-Mini 1240) set at 238 nm, with the percent release of drug calculated. Comparison of the corresponding dissolution profiles (i.e. of pure NIF and the corresponding supramolecular systems) was performed using a model-independent method and by calculation of the f_2

factor (Eq. 4). The profiles were considered similar when a resulting f_2 value was equal or higher to 50.

$$f_2 = 50\, log\left\{[1 + \frac{1}{n}\sum_{t-1}^{R}(R_t - T_t)^2]^{-0,5}\right\} x\ 100 \qquad \text{(Eq. 4)}$$

where *n* is the number of sampling points, R_t is the percentage dissolved of the reference sample (pure NIF) at each time point t, and T_t is the percentage dissolved of the studied system (supramolecular systems) at each time point t.

3. RESULTS AND DISCUSSION

3.1. Selection of auxiliary agents

The first stage of this study involved the screening and selection of the auxiliary agent (i.e. amino acid) able to produce the greatest enhancement of solubility. With this aim, the NIF solubility enhancement effect of five different AAs (Arg, Asp, Gly, His and Leu) was analysed, with the corresponding final pH of the solution being measured. The results of these studies are presented in Fig. 2A and Table 1, where the maximum NIF solubility values obtained in the presence of different AAs are shown. As depicted in Fig. 2A, the solubility of pure NIF increased in the presence of all AAs screened. As expected, the pH value of the resulting solution was different for each AA tested, with some of them eliciting almost no modification of pH value with respect to the pure NIF solution (Asp), some produced a moderate increase in the pH value (Gly and Leu) and others produced a marked increase in the resulting pH (Arg and His). It should be mentioned that both Arg and His induced an increase in the degradation rate of NIF, a fact that may be related to the relatively instability of ester compounds at higher pH values. As can be seen in Figure 2A, Asp produced the highest increase in NIF solubility among the entire set of auxiliary agents screened, exhibiting almost no modification in the pH of the solution compared to pure NIF.

Consequently, Asp was selected as the most promising auxiliary agent for the preparation of multicomponent systems containing NIF, β-CD and AA.

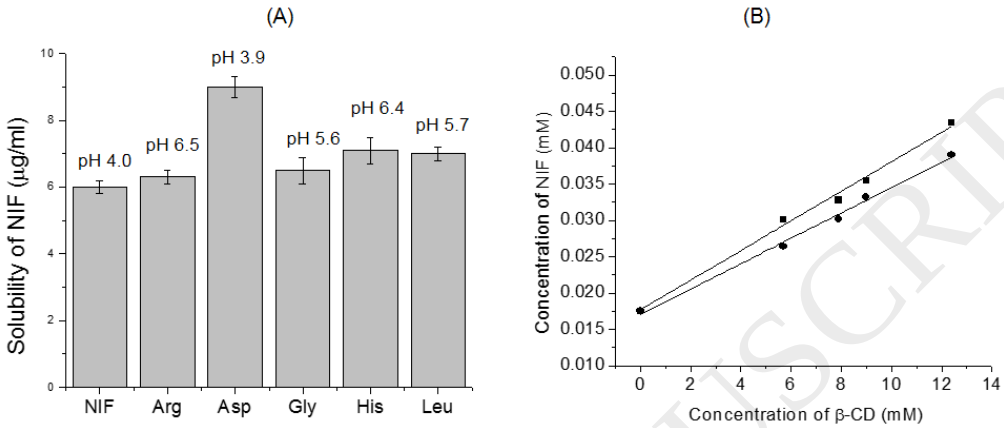

Figure 2. (A) NIF solubility in the presence of different auxiliary substances. (B) Phase solubility analysis of the binary (NIF:β-CD ●) and multicomponent (NIF:β-CD:Asp ■) systems.

3.2. Phase solubility analysis

To further study the possibility of enhancing NIF solubility by preparation of binary or multicomponent systems, complexes containing β-CD, NIF and ASP were prepared, with the corresponding phase-solubility diagrams (PSD) being determined for the NIF:β-CD complex in the presence and absence of Asp (5 mM). The corresponding results are presented in Figure 2B.The results demonstrate that the solubility of NIF increased in a linear mode, both in the binary (NIF:β-CD) and the multicomponent (NIF:β-CD:Asp) systems, and thus corresponded to the type A_L profile established by Higuchi and Connors (Higuchi & Connors, 1965), which is related to the formation of a soluble inclusion complex. The slope value in each of these diagrams was lower than 1, suggesting the formation of a

complex with 1:1 stoichiometry in the presence and absence of auxiliary agent. The corresponding affinity constant (K_C), maximum solubility (S_{max}) and efficiency of solubility (ES, S_{max}/S_0) values were calculated from each PSD and are presented in Table 1.The multicomponent system with ASP showed a K_C and ES value higher than that of the binary system. This result demonstrates cooperativity in the interaction between NIF and β-CD in the presence of Asp, a phenomenon that favours both the solubilizing and complexing ability of β-CD. These observations suggest the formation of a multicomponent complex between these substances.

3.3. Molecular modelling of binary and multicomponent complexes

It has been previously reported that auxiliary agents can increase the aqueous solubility of drugs by interacting with the external surface of the drug:CD complexes, and the observed solubility enhancement was attributable to the contribution of different interactions (van der Waal forces, formation of hydrogen bonds, hydrophobic interactions, dipole−dipole electrostatic bonds)(Loftsson & Brewster, 2012). To elucidate the structure of the complexes and to gain insight into the intermolecular interactions taking place in solution between NIF, β-CD and Asp, we performed detailed molecular modelling studies, including molecular docking and molecular dynamics simulations. Taking into account that spectroscopic data was obtained using DMSO as solvent and that solubility phase analyses were performed in aqueous solutions, in a first stage the agreement between the MD trajectories obtained in both solvents was studied. No significant differences in the conformational properties and associated interaction energies were found when simulations performed in DMSO or water were compared (Table S1, Figures S1 and S2).

First, molecular docking studies were performed in order to elucidate the lowest energy binding mode of NIF to β-CD. Ten different binding modes were obtained, which where afterwards subjected to explicit solvent MD studies and the corresponding interactions

energies were calculated. Figure 3A presents the lowest energy binding mode, with Table 2 reporting the corresponding energetic components of interaction. As can be seen, the aromatic ring containing the nitro moiety was deeply buried in theβ-CD cavity, with the Van der Waals interaction energy as the main driving force for stabilizing the complex. The overall interaction energy for the binary complex was -18.7 Kcal/mol.

Next, the multicomponent system was modelled by docking aspartic acid to the above described NIF:β-CD complex. Again, multiple binding modes were obtained, which were subjected to explicit solvent MD studies. In order to identify the most stable multicomponent system, the affinity interaction energy of NIF with the rest of the system was calculated. Figure 3B shows the predicted three dimensional structure of the multicomponent system, in which it can be seen that Asp was positioned towards the wide rim of β-CD, between the macromolecule and NIF. The resulting complex was subjected to MD analysis, revealing that described binding mode of Asp was conserved. The corresponding interaction energies for NIF were calculated in the multicomponent system (Table 2). As can be seen, the interaction of NIF with the multicomponent system is considerably more stable than that observed for the binary complex, originated in both a higher Van der Waals and electrostatic interaction. The higher Van der Waals component was mostly derived in a more stable buried conformation of the aromatic ring of NIF within the βCD hydrophobic cavity (Figure S3). In addition, Asp was able to act as a molecular bridge between NIF and βCD establishing hydrogen bond interactions as is shown in Figure S4.

A)

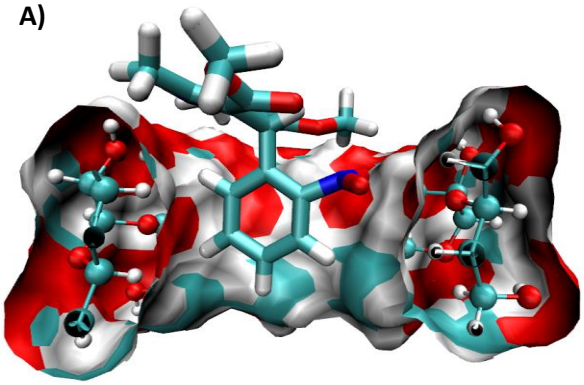

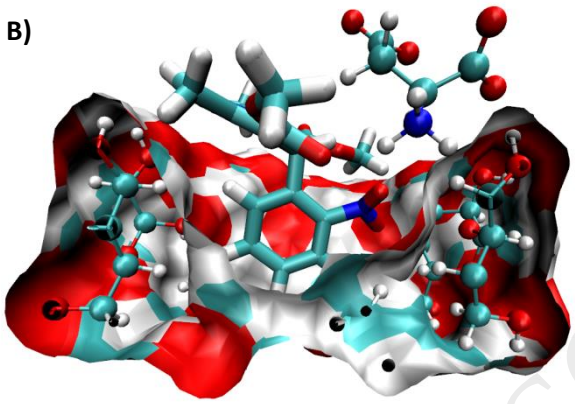

Figure 3. Three-dimensional conformation of the complexes obtained by molecular docking. (A) NIF:β-CD and (B) NIF:β-CD:ASP.

Regarding the interaction mode of NIF in both systems, it is noteworthy that the nitro group is not able to establish hydrogen bond interactions with β-CD, mostly due to an unfavourable geometry resulting from the inclusion of the aromatic ring. In addition, and based on structural parameters, CH-pi interactions between the aromatic ring of NIF and β-CD are feasible (Fig. S5 a-d), although the applied force field does not account for this type of interactions.

3.4. Proton Nuclear Magnetic Resonance spectroscopy (^{1}H NMR)

^{1}H NMR experiments were performed to further investigate the interactions between the components in solution and confirm the geometry of the inclusion complexes predicted by molecular modelling. The formation of the complexes was evidenced by comparing the changes of the chemical shift values (δ) in the ^{1}H NMR spectra of binary (NIF:β-CD) and multicomponent (NIF:β-CD:Asp) complexes, in reference with pure NIF, β-CD and Asp

spectra under the same experimental conditions. As can be seen in Table 3 and Fig. S6 (for NMR signal notation see Fig. 1), all signals of the compounds suffered – to a greater or lesser extent – a variation (Δδ), which allowed us to predict the existence of numerous interactions between the molecules that form each complex.

As can be observed in Table 3, almost all NIF proton resonances were modified, in the binary and multicomponent complexes, and exhibited a shielding effect with respect to those of the pure drug. The proton H_b and H_e of NIF showed a major displacement that can be attributed to this moiety that was located in a rich electronic density environment (proximate to the glycosidic linkage oxygen of β-CD that are rich in π electrons, for example) that produced a shielding effect. This mode of inclusion is in good agreement with the molecular modelling prediction. In addition, the upfield shift experiments for the other protons of the drug may reflect some conformational changes produced by the inclusion.

When spectra of β-CD were analysed, it was possible to observe a deshielding effect in all macromolecules protons. The downfield displacements found for both H_3 and H_5 protons (located in the interior of CD cavity), suggested the insertion of an electronegative moiety of the guest into the β-CD hydrophobic cavity, which produced the deshielding effects we observed. These findings are in agreement with the results of the theoretical studies that suggested the insertion of the aromatic ring containing the nitro group. It is important to note the great variation of hydroxyl proton signals (OH_2, OH_3 and OH_6) of β-CD. This allowed us to suggest the existence of hydrogen bond interactions with the drug. On the other hand, in the multicomponent complex, Asp could also interact with the external surface of β-CD, because the protons H_{II} exhibited deshielding effects, which might be explained by the presence of hydrogen bond interactions between the amino acid and β-CD. The displacement of the protons was more apparent in the NIF:β-CD:Asp multicomponent complex, and confirmed the formation of a more stable complex in the presence of Asp. The

results obtained in the NMR studies are in agreement with the observation of phase solubility analysis and with the geometries suggested for the molecular modelling assays.

3.5. Infrared Spectroscopy (FTIR)

To evaluate any possible interaction of the drug with β-CD and Asp molecules in the solid state, the FTIR technique was employed. In Figure S7 the infrared spectra of pure compounds as well as NIF:β-CD and NIF:β-CD:Asp systems (both PM and KN) are shown. NIF spectra showed peaks at 3330 cm^{-1} (N-H aromatic), 3101 cm^{-1} (C-H aromatic), 2952 cm^{-1} (C-H aliphatic), 1685 cm^{-1} (C=O), 1529 cm^{-1} (NO_2), 1495 cm^{-1} (C=C aromatic) and 1227 cm^{-1} (C-C-O ester). Since no new peaks were observed when the FTIR spectra for the binary (PM and KN) and multicomponent (PM and KN) systems were compared with those of the pure compounds, the formation of covalent interactions was discarded. In addition, no important changes were observed in the spectra of either PM (Table 4), since the main peaks related to functional groups of the involved substances were maintained. In the case of systems prepared by KN, a shift of various absorption bands of NIF was observed, compared with the pure drug (Table 4). This would indicate that these functional groups could be involved in interactions necessary for the formation of the complexes in solid state.

3.6. Differential Scanning Calorimetry (DSC) and Thermogravimetry (TG)

The thermal properties of the supramolecular systems were evaluated by means of TG and DSC, and were compared with the pure compounds. The relative degree of NIF crystallinity in systems was calculated based on melting enthalpy. The TG and DSC curves of all samples studied are depicted in Figure 4. The DSC and TG curves of pure NIF showed a sharp endothermic peak at 173°C, attributable to the melting process of the crystalline form of the drug, followed by its thermal decomposition (228 °C, 99% mass loss). For β-CD, two

important events were observed: the first was an endothermic peak between 50 and 105°C (7.6% mass loss) and the second (308°C, 79.9% mass loss) was attributable to dehydration and decomposition, respectively. Asp curves showed a single stage of mass loss attributable to it degradation at 234 °C. In the analysis of DSC and TG curves of binary and multicomponent physical mixtures, no significant changes were observed and the crystallinity degree of NIF was not modified. On the other hand, the NIF:β-CD complex, prepared by the kneaded method, exhibited a small decrease of drug crystallinity (RDC: 91%) while the NIF:β-CD:Asp complex showed a substantial reduction of drug crystallinity (RDC: 56%), indicating a significant concentration of the drug in its amorphous form, reinforcing the multicomponent complex formation.

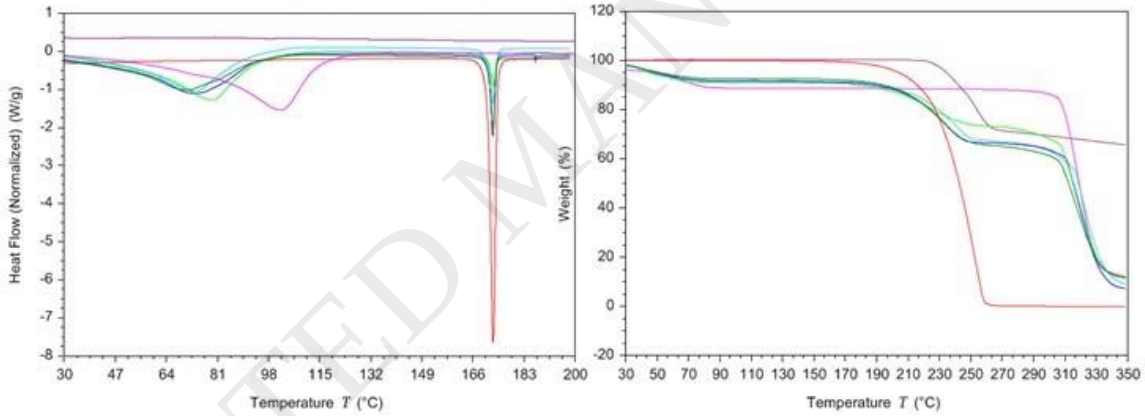

Figure 4.DSC and TG curves of: NIF (red), β-CD (pink), Asp (purple), NIF:β-CD PM system (blue), NIF:β-CD KN system (light blue), NIF:β-CD:Asp PM system (green) and NIF:β-CD:Asp KN system (light green).

3.7. Powder X-ray diffraction (PXRD)

PXRD was employed to study the effect of binary and multicomponent complexation of NIF by cyclodextrin on their crystalline structures. The diffractograms of NIF, βCD, Asp physical mixtures and the corresponding inclusion complexes are presented in Fig. 5A.The PXRD

patterns of NIF (8.2, 10.5, 11.7, 16.3, 24.4, 26), βCD (10.7, 12.6, 15.5, 17.2, 20.8 and 27.2) and Asp (11.8, 21.7, 22.8, 23.4 and 28.2) show intense sharp peaks that indicates a high crystallinity. In addition, it was possible to observe the presence of all the characteristic peaks of pure compounds in the diffractograms corresponding to the binary and multicomponent systems prepared by PM, evidencing that complexation between them did not occurred. In contrast, in the NIF:βCD and NIF:βCD:Asp systems obtained by KN, a decrease in the crystallinity degree of the compounds was observed, although some characteristic peaks of pure NIF were still detectable. The results obtained by PXRD and DSC and the observed low crystallinity state of the systems obtained by KN confirms the host-gest interactions in the solid state, strongly supporting the formation of inclusion complexes.

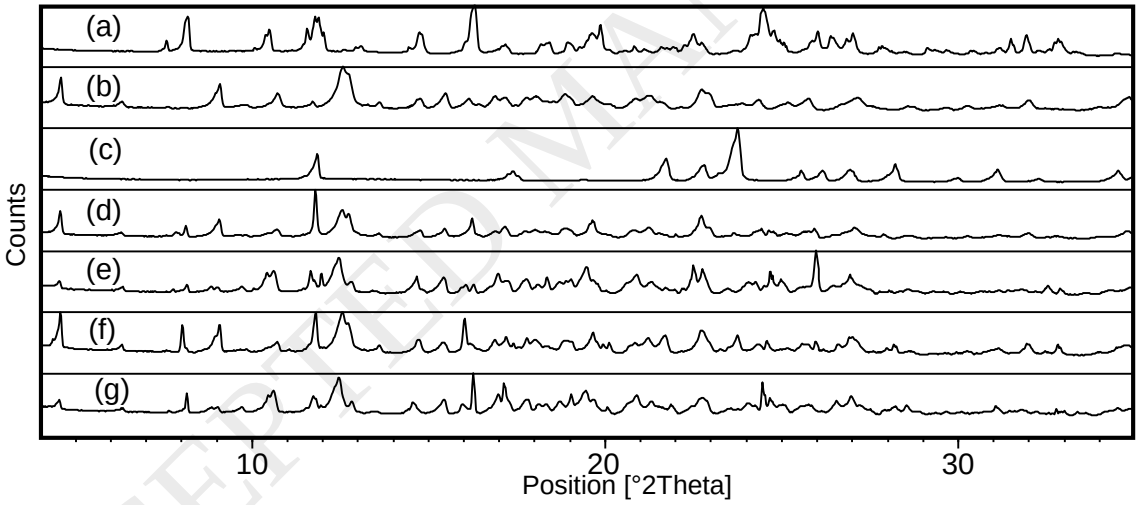

(B)

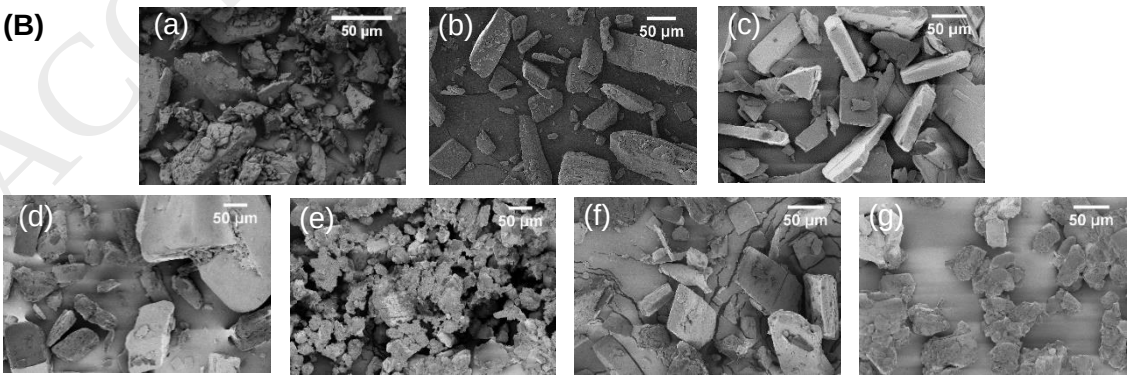

Figure 5. (A) Powder X-ray diffractograms of: (a) NIF, (b) β-CD, (c) Asp, (d) NIF:β-CD PM system (e) NIF:β-CD KN system, (f) NIF:β-CD:Asp PM system and (g) NIF:β-CD:Asp KN system. **(B)** Scanning electron microphotographs of: (a) NIF, (b) β-CD, (c) Asp, (d) NIF:β-CD PM system (e) NIF:β-CD KN system, (f) NIF:β-CD:Asp PM system and (g) NIF:β-CD:Asp KN system.

3.8. Scanning Electron Microscopy (SEM)

SEM was used to evaluate the morphological characteristics of the individual compounds, their physical mixtures and corresponding complexes. The representative SEM images of all materials are shown in Figure 5B. In both systems prepared by PM, the size and shape of the particles were more varied and irregular than those obtained by the KN method. In the NIF:β-CD KN complex, it was possible to observe bulky and dense blocks, while more homogenous particle size distribution was observed in the NIF:β-CD:Asp KN complex.

3.9. Dissolution study

The dissolution studies were performed for pure NIF, and for both binary and multicomponent systems obtained by PM and KN methods with the aim to evaluate the effect of complexation on the drug dissolution rate. The results of the dissolution study are shown in Figure 6. The study showed 28 ± 2% dissolution of pure NIF in the initial 5 minutes, and a maximum of 30 ± 2% drug dissolution at 180 minutes. This poor dissolution of NIF can be attributed to the lower solubility of NIF in the dissolution medium. No differences were observed when unprocessed drug was compared with the pure drug submitted to the kneading process (NIF KN 27.7 ± 0.4% and 39 ± 2%, at 5 and 180 min, respectively, with an f_2 value of 68). Both binary (NIF:β-CD) and multicomponent (NIF:β-CD:Asp) complexes significantly improved the dissolution profile of NIF, and the profiles were not similar to that of the pure drug. The improvement in drug release was, in order, pure NIF = NIF KN (f_2: 68)

< binary PM (f_2: 39) < binary KN (f_2: 32) < multicomponent PM (f_2: 29) < multicomponent KN (f_2: 22). The percentage of release shown by the systems at 180 minutes was 68 ± 2% (binary PM), 66 ± 6% (binary KN), 79 ± 1% (multicomponent PM) and 95.0 ± 0.5% (multicomponent KN); which implied an increase of 2.2, 2.2, 2.6 and 3.1 times, respectively. The fact that the multicomponent complexes improved the dissolution profile of NIF, not only with respect to the pure drug, but also to the binary complexes, confirms the ability of Asp to act as an auxiliary agent to permit optimization of drug dissolution behaviour. The difference found between the profiles of NIF:β-CD:Asp PM and NIF:β-CD:Asp KN (f_2:43) are attributable to the fact that the drug is partially amorphized in the NIF:β-CD:Asp KN, as was demonstrated by the DSC and PXRD results.

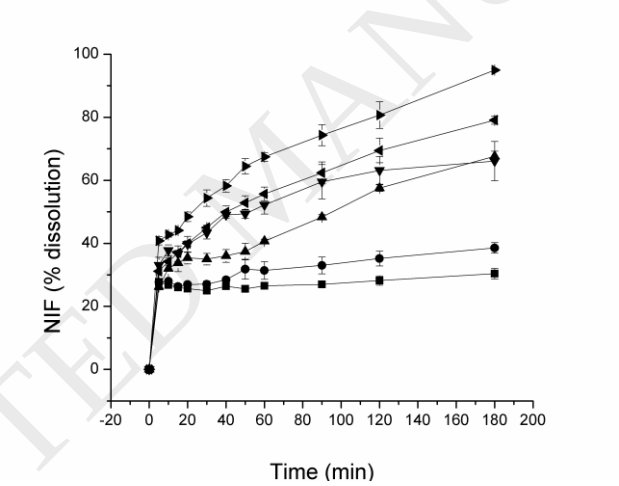

Figure 6. Dissolution profiles of pure NIF (■) and NIF kneading (●), NIF:β-CD physical mixture (▲), NIF:β-CD kneading system (▼), NIF:β-CD:Asp physical mixture (◄) and NIF:β-CD:Asp kneading system (►).

CONCLUSIONS

This study shows that the formation of a multicomponent complex between NIF, β-CD and Asp was an adequate approach to improve the solubility and dissolution performance of the drug. Computational studies revealed that the aromatic ring of the drug was deeply buried

in the β-CD cavity, and the Van der Waals interaction energy was the main driving force for the stabilization of the complex. In addition, computational modelling studies revealed that Asp increased the stability of the multicomponent complex, which was consistent with the experimental finding observed in the phase solubility analysis and ^{1}H NMR studies. The observed enhancement in the affinity of NIF in the multicomponent system is originated in a more stable inclusion of the aromatic ring of NIF within the βCD cavity, and that results in a significantly higher VDW interaction. The auxiliary agent is anchored facing the wide rim of βCD in the interface between the host and guest molecules, acting as a bridge for electrostatic interaction between them. Changes in shape and size distribution of NIF in the multicomponent complex were evident by SEM. In addition, the DSC and PXRD data confirmed a greater decrease in the NIF crystallinity in the multicomponent complex, compared to the binary one. Although all of the systems studied have improved the dissolution rate of NIF, largely, the multicomponent complex was superior to all other systems. Therefore, we conclude that the NIF:β-CD:Asp multicomponent complex will be valuable to optimize the properties of NIF pharmaceutical formulations.

Acknowledgments

The authors wish to acknowledge the assistance of the Consejo Nacional de Investigaciones Científicas y Técnicas (CONICET), the Universidad Nacional de Córdoba, Fondo para la Investigación Científica y Tecnológica (FONCyT) Préstamo BID PICT 2013-2150, and the Secretaría de Ciencia y Técnica de la Universidad Nacional de Córdoba (SECyT) which provided support and facilities for this investigation. We also thank Ferromet S.A. (agent of Roquette in Argentina) for its donation of β-cyclodextrin. We are grateful to Dr. Gloria Bonetto for NMR measurements and for her helpful discussions on the ^{1}H NMR spectra. M.A.Q, M.R.L. and A.Z. are career research members of CONICET.

REFERENCES

Acartürk, F., Kişlal, Ö., & Çelebi, N. (1992). The effect of some natural polymers on the solubility and dissolution characteristics of nifedipine. *International Journal of Pharmaceutics, 85*(1), 1-6.

Aiassa, V., Zoppi, A., Albesa, I., & Longhi, M. R. (2015). Inclusion complexes of chloramphenicol with β-cyclodextrin and aminoacids as a way to increase drug solubility and modulate ROS production. *Carbohydrate Polymers, 121*, 320-327.

Aiassa, V., Zoppi, A., Becerra, M. C., Albesa, I., & Longhi, M. R. (2016). Enhanced inhibition of bacterial biofilm formation and reduced leukocyte toxicity by chloramphenicol:β-cyclodextrin:N-acetylcysteine complex. *Carbohydrate Polymers, 152*, 672-678.

Barbosa, J. A. A., Zoppi, A., Quevedo, M. A., de Melo, P. N., de Medeiros, A. S. A., Streck, L., de Oliveira, A. R., Fernandes-Pedrosa, M. F., Longhi, M. R., & da Silva-Júnior, A. A. (2014). Triethanolamine stabilization of methotrexate-β-cyclodextrin interactions in ternary complexes. *International Journal of Molecular Sciences, 15*(9), 17077-17099.

Bayomi, M. A., Abanumay, K. A., & Al-Angary, A. A. (2002). Effect of inclusion complexation with cyclodextrins on photostability of nifedipine in solid state. *International Journal of Pharmaceutics, 243*(1), 107-117.

Beig, A., Miller, J. M., & Dahan, A. (2013). The interaction of nifedipine with selected cyclodextrins and the subsequent solubility–permeability trade-off. *European Journal of Pharmaceutics and Biopharmaceutics, 85*(3, Part B), 1293-1299.

Case, D. A., Cerutti, D. S., Cheatham Iii, T. E., Darden, T. A., Duke, R. E., Giese, T. J., & Kollman, P. A. (2018). AMBER 2018. University of California, San Francisco.

Chutimaworapan, S., Ritthidej, G. C., Yonemochi, E., Oguchi, T., & Yamamoto, K. (2000). Effect of water-soluble carriers on dissolution characteristics of nifedipine solid dispersions. *Drug Development and Industrial Pharmacy, 26*(11), 1141-1150.

de Araújo, M. V. G., Vieira, J. V. F., da Silva, C. W. P., Barison, A., Andrade, G. R. S., da Costa, N. B., Barboza, F. M., Nadal, J. M., Novatski, A., Farago, P. V., & Zawadzki, S. F. (2017). Host-guest complexes of 2-hydroxypropyl-β-cyclodextrin/β-cyclodextrin and nifedipine: 1H NMR, molecular modeling, and dissolution studies. *Journal of Molecular Structure, 1150*, 146-154.

Filipović-Grčić, J., Bećirević-Laćan, M., Skalko, N., & Jalšenjak, I. (1996). Chitosan microspheres of nifedipine and nifedipine-cyclodextrin inclusion complexes. *International Journal of Pharmaceutics, 135*(1), 183-190.

Frisch, M. J., Trucks, G. W., Schlegel, H. B., Scuseria, G. E., Robb, M. A., Cheeseman, J. R., Scalmani, G., Barone, V., Mennucci, B., Petersson, G. A., Nakatsuji, H., Caricato, M., Li, X., Hratchian, H. P., Izmaylov, A. F., Bloino, J., Zheng, G., Sonnenberg, J. L., Hada, M., Ehara, M., Toyota, K., Fukuda, R., Hasegawa, J., Ishida, M., Nakajima, T., Honda, Y., Kitao, O., Nakai, H., Vreven, T., Montgomery, J. A., Peralta, J. E., Ogliaro, F., Bearpark, M., Heyd,

J. J., Brothers, E., Kudin, K. N., Staroverov, V. N., Kobayashi, R., Normand, J., Raghavachari, K., Rendell, A., Burant, J. C., Iyengar, S. S., Tomasi, J., Cossi, M., Rega, N., Millam, J. M., Klene, M., Knox, J. E., Cross, J. B., Bakken, V., Adamo, C., Jaramillo, J., Gomperts, R., Stratmann, R. E., Yazyev, O., Austin, A. J., Cammi, R., Pomelli, C., Ochterski, J. W., Martin, R. L., Morokuma, K., Zakrzewski, V. G., Voth, G. A., Salvador, P., Dannenberg, J. J., Dapprich, S., & Daniels, A. D. (2009).

Gajendran, J., Krämer, J., Shah, V. P., Langguth, P., Polli, J., Mehta, M., Groot, D. W., Cristofoletti, R., Abrahamsson, B., & Dressman, J. B. (2015). Biowaiver Monographs for Immediate-Release Solid Oral Dosage Forms: Nifedipine. *Journal of Pharmaceutical Sciences, 104*(10), 3289-3298.

Göke, K., Lorenz, T., Repanas, A., Schneider, F., Steiner, D., Baumann, K., Bunjes, H., Dietzel, A., Finke, J. H., Glasmacher, B., & Kwade, A. (2018). Novel strategies for the formulation and processing of poorly water-soluble drugs. *European Journal of Pharmaceutics and Biopharmaceutics, 126*, 40-56.

Heydari, A., Iranmanesh, M., Doostan, F., & Sheibani, H. (2015). Preparation of Inclusion Complex Between Nifedipine and Ethylenediamine-β-Cyclodextrin as Nanocarrier Agent. *Pharmaceutical Chemistry Journal, 49*(9), 605-612.

Higuchi, T., & Connors, K. (1965). Phase Solubility Tecniques. *Adv in Analitical Chemistry and Instrumentation. Interscience, 4*, 117-212.

Humphrey, W., Dalke, A., & Schulten, K. (1996). VMD: Visual molecular dynamics. *Journal of Molecular Graphics, 14*(1), 33-38.

Iacovino, R., Caso, J. V., Di Donato, C., Malgieri, G., Palmieri, M., Russo, L., & Isernia, C. (2017). Cyclodextrins as complexing agents: Preparation and applications. *Current Organic Chemistry, 21*(2).

Jagdale, S. C., Jadhav, V. N., Chabukswar, A. R., & Kuchekar, B. S. (2012). Solubility enhancement, physicochemical characterization and formulation of fast-dissolving tablet of nifedipine-betacyclodextrin complexes. *Brazilian Journal of Pharmaceutical Sciences, 48*(1), 131-145.

Kawabata, Y., Wada, K., Nakatani, M., Yamada, S., & Onoue, S. (2011). Formulation design for poorly water-soluble drugs based on biopharmaceutics classification system: Basic approaches and practical applications. *International Journal of Pharmaceutics, 420*(1), 1-10.

Kirschner, K. N., Yongye, A. B., Tschampel, S. M., González-Outeiriño, J., Daniels, C. R., Foley, B. L., & Woods, R. J. (2008). GLYCAM06: a generalizable biomolecular force field. Carbohydrates. *Journal of Computational Chemistry, 29*(4), 622-655.

Loftsson, T., & Brewster, M. E. (2012). Cyclodextrins as functional excipients: Methods to enhance complexation efficiency. *Journal of Pharmaceutical Sciences, 101*(9), 3019-3032.

Martínez, L., Andrade, R., Birgin, E. G., & Martínez, J. M. (2009). PACKMOL: A package for building initial configurations for molecular dynamics simulations. *Journal of Computational Chemistry, 30*(13), 2157-2164.

MarvinSketch. (2017). MarvinSketch v.16.2.15. ChemAxon Ltd.

Mercuri, A., Fares, R., Bresciani, M., & Fotaki, N. (2016). An in vitro–in vivo correlation study for nifedipine immediate release capsules administered with water, alcoholic and non-alcoholic beverages: Impact of in vitro dissolution media and hydrodynamics. *International Journal of Pharmaceutics, 499*(1), 330-342.

Miller, B. R., McGee, T. D., Swails, J. M., Homeyer, N., Gohlke, H., & Roitberg, A. E. (2012). MMPBSA.py: An efficient program for end-state free energy calculations. *Journal of Chemical Theory and Computation, 8*(9), 3314-3321.

Morris, G. M., Ruth, H., Lindstrom, W., Sanner, M. F., Belew, R. K., Goodsell, D. S., & Olson, A. J. (2009). Software news and updates AutoDock4 and AutoDockTools4: Automated docking with selective receptor flexibility. *Journal of Computational Chemistry, 30*(16), 2785-2791.

Muankaew, C., & Loftsson, T. (2018). Cyclodextrin-Based Formulations: A Non-Invasive Platform for Targeted Drug Delivery. *Basic & Clinical Pharmacology & Toxicology, 122*(1), 46-55.

Narayanan, G., Boy, R., Gupta, B. S., & Tonelli, A. E. (2017). Analytical techniques for characterizing cyclodextrins and their inclusion complexes with large and small molecular weight guest molecules. *Polymer Testing, 62*, 402-439.

Nikolić, V., Ilić, D., Nikolić, L., Stanković, M., Cakić, M., Stanojević, L., Kapor, A., & Popsavin, M. (2010). The protection of nifedipin from photodegradation due to complex formation with β-cyclodextrin. *Central European Journal of Chemistry, 8*(4), 744-749.

Škalko, N., Brandl, M., Bećirević-Laćan, M., Filipović-Grčić, J., & Jalšenjak, I. (1996). Liposomes with nifedipine and nifedipine-cyclodextrin complex: calorimetrical and plasma stability comparison. *European Journal of Pharmaceutical Sciences, 4*(6), 359-366.

Uekama, K., Ikegami, K., Wang, Z., Horiuchi, Y., & Hirayama, F. (1992). Inhibitory effect of 2-hydroxypropyl-beta-cyclodextrin on crystal-growth of nifedipine during storage: superior dissolution and oral bioavailability compared with polyvinylpyrrolidone K-30. *J Pharm Pharmacol, 44*(2), 73-78.

Vieira, A. C. C., Ferreira Fontes, D. A., Chaves, L. L., Alves, L. D. S., de Freitas Neto, J. L., de La Roca Soares, M. F., Soares-Sobrinho, J. L., Rolim, L. A., & Rolim-Neto, P. J. (2015). Multicomponent systems with cyclodextrins and hydrophilic polymers for the delivery of Efavirenz. *Carbohydrate Polymers, 130*, 133-140.

Wang, J., Wolf, R. M., Caldwell, J. W., Kollman, P. A., & Case, D. A. (2004). Development and testing of a general Amber force field. *Journal of Computational Chemistry, 25*(9), 1157-1174.

Table

Table 1. Effect of the amino acids and β-CD on NIF solubility.

System	S_{max}*(μg/ml)*[a]	*ES*[b]	K_C *(M^{-1})*	*pH*
Arg	6.3 ± 0.2	1.1	-	6.5
Asp	9.0 ± 0.3	1.5	-	3.9
Gly	6.5 ± 0.6	1.1	-	5.6
His	7.1 ± 0.8	1.2	-	6.4
Leu	7.0 ± 0.2	1.2	-	5.7
β-CD	13.5 ± 0.2	2.2	99± 2	4.0
β-CD:Asp	15.0 ± 0.2	2.5	117± 4	4.0

[a]S_{max}, maximum value of solubility measured; [b]ES, efficiency of solubility (S_{max}/S_0), S_0= 6.06 ± 0.02 μg/ml.

Table 2. Total Interaction energy (ΔE global) and corresponding components (VDW, Van der Waals energy; EEL, electrostatic energy; EGB, polar desolvation energy, ESURF, non-polar solvation energy) for the interaction of NIF with βCD and βCD:Asp systems, respectively.

System	*VDW*	*EEL*	*EGB*	*ESURF*	*ΔE global*
NIF:β-CD	-29.0 (±3.2)	-5.5(±1.3)	19.5 (±4.5)	-3.7 (±0.2)	-18.7 (±3.3)
NIF:β-CD:Asp	-42.5 (±2.7)	-24.2 (±5.6)	39.3 (±5.0)	-4.6 (±0.1)	-31.9 (±2.8)

Table 3. Chemical shifts of protons of pure NIF, β-CD and Asp in free and complex form.

NIF protons	*δ (ppm)*	*δ (ppm) NIF:β-CD*	*Δδ (ppm)*[a]	*δ (ppm) NIF:β-CD:Asp*	*Δδ (ppm)*[a]
H_a	9.0170	9.0170	0.0000	9.0140	-0.0030
H_b	5.4900	5.4870	-0.0030	5.4840	-0.0060
H_c	7.6925	7.6905	-0.0020	7.6905	-0.0020

H_d	7.5910	7.5890	-0.0020	7.5900	-0.0010
H_e	7.4550	7.4525	-0.0025	7.4530	-0.0020
H_f	7.3500	7.3495	-0.0005	7.3490	-0.0010
H_g	2.2490	2.470	-0.0020	2.2460	-0.0030
H_h	3.4490	3.4470	-0.0020	3.4470	-0.0020
β-CDprotons	*δ (ppm)*	*δ (ppm) NIF:β-CD*	*Δδ (ppm)[a]*	*δ (ppm) NIF:β-CD:Asp*	*Δδ (ppm)[a]*
H_1	4.8240	4.8260	0.0020	4.8265	0.0025
H_2	3.2980	3.2980	0.0000	3.3010	0.0030
OH_2	5.7215	5.7370	0.0155	5.7345	0.0130
H_3	3.6280	3.6300	0.0020	3.6320	0.0040
OH_3	5.6700	5.6825	0.0125	5.6830	0.0130
H_4	3.2750	3.2775	0.0025	3.2760	0.0010
H_5	3.5575	3.5585	0.0010	3.5595	0.0020
H_6	3.6280	3.6300	0.0020	3.6320	0.0040
OH_6	4.4500	4.4630	0.0130	4.4600	0.1000
ASP protons	*δ (ppm)*	*δ (ppm) NIF:β-CD*	*Δδ (ppm)[a]*	*δ (ppm) NIF:β-CD:Asp*	*Δδ (ppm)[a]*
H_I	3.7795	-	-	3.7790	-0.0005
$H_{II'}$	2.7150	-	-	2.7170	0.0020
$H_{II''}$	2.3830	-	-	2.3905	0.0075

Table 4. Wavenumbers (cm^{-1}) of NIF pure, binary and multicomponent systems.

Assignment	***NIF***	*NIF:β-CD$_{PM}$*	***NIF:β-CD$_{KN}$***	*NIF:β-CD:Asp$_{PM}$*	***NIF:β-CD:Asp$_{KN}$***
NH arom	**3330**	*3331*	**3332**	*3331*	**3333**
NO_2	**1529**	*1529*	**1531**	*1529*	**1530**
C=C arom	**1495**	*1495*	**1498**	*1495*	**1498**
C-C-O ester	**1227**	*1227*	**1229**	*1227*	**1229**